Journal of Japan Association for Earthquake Engineering, Vol. 25, No. 8, 2025

EFFECT OF IMPROVEMENT RANGE OF STATIC SAND COMPACTION PILE METHOD FOR LIQUEFACTION MITIGATION ON HORIZONTAL RESISTANCE OF PILES

Osamu KANEKO[1] and Hiroki YOSHITOMI[2]

[1] Member, Dr. Eng., Professor, Hiroshima Institute of Technology, Hiroshima, Japan, o.kaneko.b8@cc.it-hiroshima.ac.jp
[2] Section Manager, Geotechnical Division Engineering Department, Fudo Tetra Corporation, Tokyo, Japan, hiroki.yoshitomi@fudotetra.co.jp

ABSTRACT: The static compaction sand pile method is a method of increasing liquefaction resistance by compaction of the ground through low-noise and low-vibration construction of sand piles using static press-in force. In this paper, based on a case study of a pile-foundation building, the effect of the narrowing of the improvement area on the stresses generated by the piles was investigated by static incremental analysis using a beam-spring model that takes into account the linearity of the soil and pile materials. The analysis was performed by using the earthquake response analysis to obtain the ground displacement and horizontal pile head force, and then using the shape and pile layout of the building, and the location of the area to be improved by the static compaction sand pile method as the parameters. The results of these analyses showed that when the area of improvement is reduced, the horizontal forces are concentrated in the improved area, which requires attention to secure the shear strength of the pile, but the influence on the bending moment is relatively small, and the load on the unimproved area tends to be reduced compared to that of the fully improved area.

Keywords: *Static sand compaction pile method, Liquefaction mitigation, Pile foundation, Horizontal resistance*

1. INTRODUCTION

The static sand compaction pile method[1)] increases the ground liquefaction resistance by compacting the ground with sand piles, which are constructed using static press-in force. The principle behind this liquefaction countermeasure is that it increases ground density through the impact of vibration, or material compaction[2)]. This method can be implemented with low noise and vibration, making it appropriate for urban construction projects with an extensive track record where mitigating environmental impacts during construction is crucial.

Liquefaction countermeasures through ground improvement, including this method, enhance a specific area of the ground not only directly beneath a structure but also in its surroundings. The improvement area is extended far enough to ensure the structure's seismic stability, even if the ground

outside the improved area undergoes liquefaction. However, it has been noted that "there has been limited systematic research to determine improvement areas, and these areas have typically been estimated based on the engineering judgment of designers"[3]. Additionally, the static sand compaction pile method inherently induces ground displacement[4] due to the forced insertion of sand piles. It is particularly important to prepare a construction plan that can mitigate the impacts of ground deformation on neighboring land in close proximity to the improvement area and on underground structures near the improvement area. Therefore, the static sand compaction pile method may need to be replaced with an alternative method if construction measures[5], such as installing displacement buffer holes to absorb ground displacement and devising construction procedures to mitigate impacts on surrounding land, are insufficient to keep the impacts within an allowable range.

While improvement areas are typically determined regardless of the building's importance or size, the "Recommendations for Design of Building Foundations" by the Architectural Institute of Japan stipulate that the foundation and superstructure designs must ensure meet required performance criteria within their limit states.[6] Therefore, it can be concluded that improvement areas and specifications should be determined through detailed evaluations that carefully consider performance requirements. In pile foundation design, optimizing the improvement area and specifications to ensure the required performance of an entire structure, considering the pile arrangement and the cross-sectional performance of each pile, was assessed as an effective approach. This helps streamline pile foundation design by reducing the number of piles needed for ground improvement while minimizing impacts on surrounding land.

In this report, to assess the impact of ground improvement areas on the horizontal resistance of piles, a pile stress analysis was conducted. This analysis was based on the actual construction of buildings utilizing pile foundations, where the positional relationship between building geometrical shapes (pile arrangement) and the work ranges of the static sand compaction pile method used as a key parameter. Moreover, this study also includes an examination of the improvement area setting method that meet both design and construction requirements based on the results of the stress analysis.

2. IMPROVEMENT AREAS OF STATIC SAND COMPACTION PILE METHOD

In the static sand compaction pile method, proposals have been made for defining the improvement area (additional improvement width) to prevent negative impacts caused by the destabilization of unimproved adjacent ground. These include a simplified method[7), 8)] that limits the improvement area to 1/2 or 2/3 of the improvement depth from the external surfaces of a building, and another method[9)] that determines the improvement area based on the relationship between the active failure range induced by liquefaction in unimproved ground and the passive resistance of the improved ground adjacent to a structure. A detailed evaluation of the improvement area typically requires seepage or seismic response analysis. However, these analyses have rarely been utilized in practical design due to the challenges associated with defining input parameters appropriately. Additionally, these methods for defining improvement areas have been regarded as guidelines or principles[7)]; however, improvement areas are usually determined based on engineering judgment and experience to facilitate construction works.

Furthermore, both of the aforementioned methods for defining improvement areas often result in a wide additional outer circumferential improvement width. It may be possible to reduce the improvement area includes the strategic arrangement of crushed stone piles to dissipate excess pore pressure propagating from unimproved ground or the installation of a waterproof wall at the outermost section to prevent the propagation of excess pore pressure. Similarly, reducing the improvement area is a potential measure to address situations where the required improvement area cannot be secured due to site constrains such as proximity to adjacent land or existing structures. However, the effectiveness of reducing improvement areas has only been confirmed through numerical analyses, laboratory experiments, and past earthquakes, with insufficient data available to establish a comprehensive design method[5)]. Thus, improvement area specifications have been determined based on past experience.

Given the absence of a universally established framework for defining improvement areas, it remains challenging to standardize them based on existing knowledge. Consequently, achieving safe

and cost-effective foundation structures requires tailoring ground improvement measures to each specific project, considering both the required performance of the foundation and site-specific construction constraints.

3. ANALYSIS METHOD

3.1 Outline of Building and Ground Improvement Used in Analysis

In this study, a method for determining improvement areas for the static sand compaction pile method was examined by applying analytical conditions based on the design data of a 22–story reinforced concrete (RC) building without a basement, constructed in Hiroshima City.

According to the piling plan shown in Fig. 1, 24 cast-in-place RC piles with enlarged bases are installed beneath the columns. Each pile has a strength of Fc30, a length of 32 m, and pile heads positioned at GL−4.7 m. The cross-sectional properties at axial sections and reinforcement bar arrangement of these piles were designed to ensure they can withstand bending moments and shear forces up to, but not exceeding, their ultimate bending moment and ultimate shear strength in the event of large, infrequent earthquakes (classified as Level 2 earthquakes). The pile specifications in Table 1 show that circumferential piles (P2), which experience significant variable axial forces during earthquakes, contain more reinforcement bars than other piles.

Figure 2 represents the typical boring investigation results conducted at seven locations on the premises (the ground displacement indicated in the figure will be explained later). The ground consists of a medium to fine silty sand layer with a relatively large variation in *N*-values, ranging from 3 to 12, from the surface to GL−12.3 m, and a groundwater level at GL−3.5 m. Beneath this layer, there is a silt layer with *N*-values ranging from 3 to 5, as well as a silty sand layer with an *N*-value of approximately 10, both of which have a lower potential for liquefaction. The sand and gravel layer, which serves as the bearing layer for the piles, is located at a depth of GL−34 m or deeper. Figure 3 depicts the liquefaction assessment results, achieved using the method specified in “Recommendations for Design of Building Foundations”[10] by Architectural Institute of Japan for the ground depths down to GL−12 m. For ground surface horizontal acceleration of α_{max} = 1.8 m/s^2 (with a local factor of 0.9), the ground at depths from GL−6 to −8 m and from GL−10 to −12 m had safety factors (F_L) less than 1.0. For α_{max} = 3.5 m/s^2, F_L was 1.0 or less in all layers down to GL−12 m. These results indicate that the ground down to GL−12 m is considered to have a potential for liquefaction. Therefore, the static sand compaction pile method as a countermeasure against liquefaction was implemented. Sand piles were arranged directly beneath the building in a grid pattern at 1.7 m intervals (with an improvement rate of 13.3%) to achieve F_L greater than 1.0 in all layers for α_{max} = 1.8 m/s² and an average F_L greater than 1.0 for α_{max} = 3.5 m/s². Additionally, crushed stone piles were arranged in two rows along the circumferential section to mitigate the negative impacts of the surrounding unimproved ground, which is prone to liquefaction. The improvement length was set to 12.3 m, consisting of a 4.7 m section without sand and a 7.6 m section with sand.

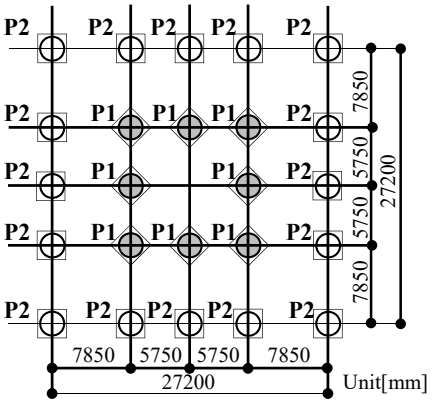

Fig. 1 Piling plan

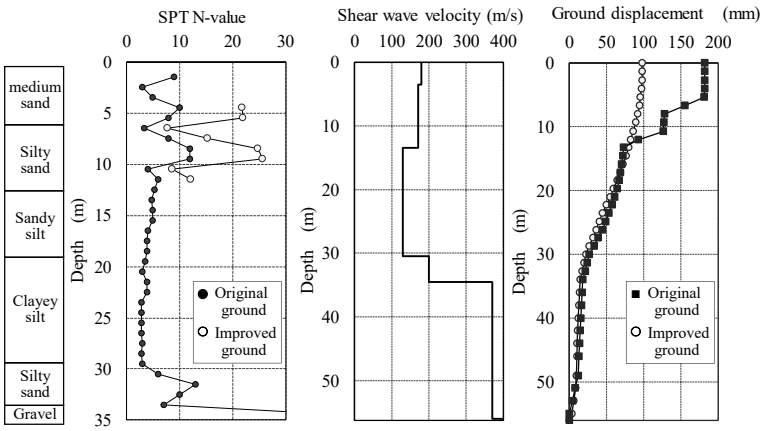

Fig. 2 Boring investigation results and ground displacement

Table 1 Pile specifications

	Diameter*1	Main reinforcement*2	Shear reinforcement*2	Number of piles
P1	2300 mm	35–D35	D13@150	8
	3500 mm	18–D35	D13@300	
P2	2300 mm	64–D35	D13@150	16
	3200 mm	40–D35	D13@300	

*1 Upper : Shaft part, Lower : Enlarged base, *2 Upper : Pile head, Lower : Shaft part

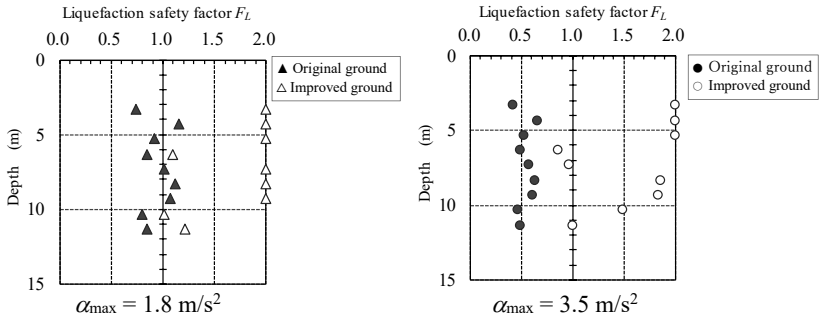

Fig. 3 Liquefaction assessment results

3.2 Analysis Method

For the stress analysis, a pushover analysis[11] using a beam–spring model was employed. In the model, the sections of the piles deeper than the foundation beams were modeled as linear members (beam elements), while the ground was modeled by spring elements. As illustrated in Fig. 4, the analysis model connects a total of 24 piles, including those installed within the improvement area (improved ground section) and those installed outside the improvement area (unimproved ground section), through rigid foundation beams. In the model, each pile is assigned ground springs and ground displacement values based on the ground conditions at the corresponding depths. Each pile is divided into elements with varying lengths: 0.5 m in the upper 10 m section from the pile head, 1.0 m in the 10 m intermediate section beneath the upper section, and 3.0 m in the section below the intermediate section. Additionally, each pile has a pinned support at the pile tip and a rigid connection at the pile head, with a degree of fixation of 1.0.

The ground springs were modeled using Eqs. (1) and (2), based on the method proposed by Mase and Nakai[12], to approximate the hyperbolic load–deformation (p–y) relationships for each layer shown in Table 2 using multiple polylines.

$$\frac{P(R)}{\delta(R)} = \frac{K_0}{1 + \frac{K_0}{P_y R}\frac{(1-R_e)}{u}\frac{2}{\pi}\ln\left\{\sec\left(\frac{\langle R-R_e\rangle}{1-R_e}\frac{\pi}{2}\right)\right\}} \quad (1)$$

$$K_0 = 1.3\frac{E_s}{(1-\nu^2)}\left(\frac{E_s B^4}{EI}\right)^{1/12} \quad (2)$$

where P is the subgrade reaction, σ is the horizontal displacement, K_0 is the initial stiffness, P_y is the plastic subgrade reaction, R is the normalized yield ratio expressed as $P(R)/P_{max}$, $\langle R\rangle$ equals R when $R \geq 0$ and 0 when $R<0$, R_e is the elastic limit R value (0 in this case), u is a constant representing the proximity to the ultimate subgrade reaction, E_s is the deformation modulus of the ground calculated from the V_s value in Fig. 2, ν is Poisson's ratio, B is the pile diameter and EI is the bending stiffness of the pile.

The internal friction angle, ϕ, and cohesion, c, used to calculate the plastic horizontal subgrade reaction[13] were determined from N-values using the experimental equations ($\phi = \sqrt{20N_1} + 20$, $c = q_u/2 = 12.5N/2$, where N_1 is the equivalent N-value corrected for effective overburden stress, and q_u is the uniaxial compressive strength)[14), 15)]. Regarding the constant u, when u = 1500, the p–y relationship closely resembles a bilinear model. When u = 150, the p–y relationship approximates a hyperbolic model. When u = 20, the p–y relationship corresponds to soil that is likely to exhibit significant non-linear behavior. Therefore, in the analysis, u values were determined based on the proximity of each layer to the plastic horizontal subgrade reaction, P_y, considering soil properties and depths[12]. The analysis did not consider the influences of a pile group. Figure 5 illustrates the relationship between subgrade reaction and horizontal displacement, referred to as p–y relationships, for the respective springs. The figure also depicts the p–y relationship derived by setting the deformation modulus of the ground, E_s, to 700 N (kN/m²), in accordance with the Method[13] specified in "Recommendations for Design of Building Foundations" by Architectural Institute of Japan. The analysis was conducted under the basic assumption that there is no reduction in subgrade reaction across the entire area of the improved ground section. It was assumed that ground improvement had been carried out to a level sufficient to prevent the improved section from being influenced by the surrounding ground, and the compaction effect was not considered, consistent with general design methods. For comparison purposes, the analysis was also conducted for two additional cases: one where the increase in density (N-value) due to compaction, as shown in Fig. 2 and Table 2, was considered, and another where a reduction rate for the subgrade reaction (Table 2), accounting for the influence of the unimproved ground section, was applied to the piles along the outermost row in the improved ground section. For the unimproved ground section, the initial stiffness and plastic horizontal subgrade reaction were reduced for layers with potential liquefaction, as shown in Table 2, based on the relationship between corrected N-values, depths, and the reduction factor β_L[10].

Table 2 Properties of the layers of soil model

No.	Bottom depth (m)	Soil classification	N-value	V_s (m/s)	c (kN/m²)	ϕ (degree)	Constant u	Reduction factor β_L
1	5.6	Sand	9 (14)	170	−	28	40	0.2 [0.6]
2	7.2	Sand	4 (9)	170	−	24	40	0.1 [0.5]
3	10.6	Sand	9 (14)	170	−	28	40	0.2 [0.6]
4	12.3	Sand	5 (9)	170	−	25	40	0.1 [0.5]
5	18.7	Silt	4	130	25	−	20	1.0
6	29.3	Silt	3	130	20	−	20	1.0
7	33.5	Sand	10	200	−	29	40	1.0
8	40.0	Sand	60	370	−	50	100	1.0

* Values in ( ) are N-value considering compaction effect. Values in [ ] are reduction factor considering the influence of the unimproved ground.

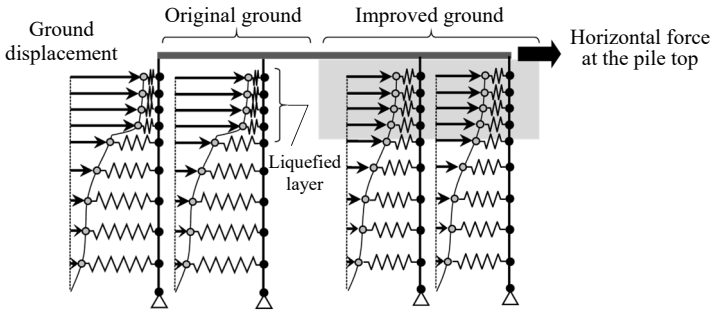

Fig. 4 Schematic view of analysis model

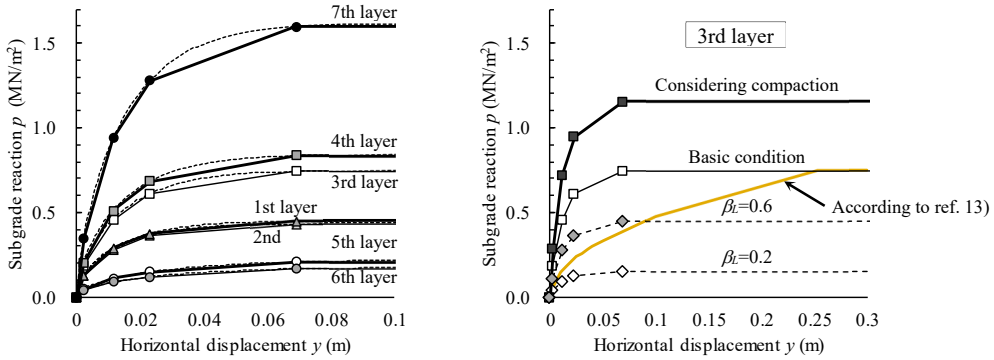

Fig. 5 Relationship between subgrade reaction and horizontal displacement

For the material characteristics of pile bodies, based on the results of cross-sectional analysis, the relationship between bending moment and curvature (M–ϕ relationship) was modeled as a trilinear representation with three breakpoints corresponding to the bending moment at cracking (M_c), yield moment (M_y), and ultimate moment (M_u). Additionally, as shown in Fig. 6(a), the piles were divided into groups based on the design values of axial force (N) under stationary load and Level 2 earthquake load, assumed to act on the piles from left to right. The M–ϕ relationships were then calculated, considering the axial force to remain constant for each group. Figure 6(b) illustrates the M–ϕ relationships for each axial force. In these relationships, axial deformation, shear deformation, and shear resistance were not taken into account.

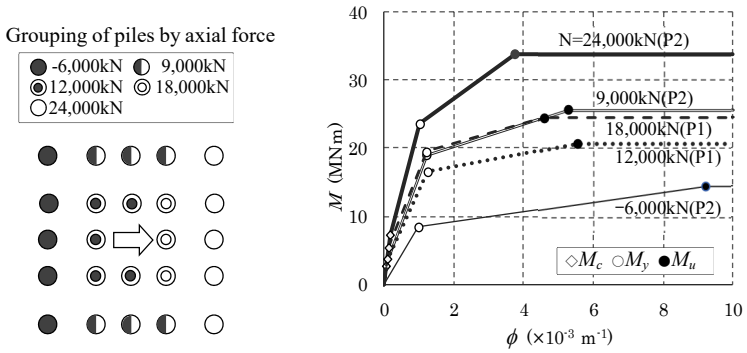

Fig. 6 Pile groups and M–ϕ relationships for each axial force

The ground displacement and horizontal force at the pile head were determined using the acceleration response spectrum (Z = 0.9) for extremely rare earthquakes (Level 2 earthquakes), as specified in Ministerial Notification No. 1461. The phase was determined based on the earthquake response analysis of the ground utilizing the non-linear step-by-step integration method. The analysis employed a simulated seismic wave with a maximum acceleration of 3.38 m/s² on free engineering bedrock, derived

from the observation record of the Tokachi-Oki Earthquake in 1968 at Hachinohe Port (NS), as the input seismic motion. The analysis was conducted using the sand-gravel layer (V_s = 540 m/s) located at GL−55 m or deeper as the engineering bedrock. Additionally, the initial ground stiffness was derived from the shear wave velocity shown in Table 2, similar to the deformation modulus of the ground, E_s, used for setting the ground springs. The effects of compaction were not considered, even after ground improvement. The non-linearity was evaluated using the R–O model, with the dynamic deformation characteristics[16] set based on the soil properties. For the ground outside the improvement area, the deformation modulus of layers with potential liquefaction was reduced using the reduction factor β_L shown in Table 2, similar to the method used for the coefficient of horizontal subgrade reaction. The ground displacement, representing the relative displacement with respect to the pile tip, was obtained from the maximum ground displacement distribution (also illustrated in Fig. 2) and applied in ten steps. For the horizontal force at the pile head, a response analysis was initially conducted using the response value at the foundation level, obtained from a separate analysis employing the equivalent bending shear model, in which a building (with a fixed foundation) was modeled as a single-story mass point system for input movement. Subsequently, the maximum foundation reaction value (51,000 kN) was applied to each pile head as a total horizontal force also distributed in ten steps in the same direction. Furthermore, the analysis included a case with a load 1.5 times greater than the Level 2 load, equivalent to Seismic Grade 3 in Japanese Housing Performance Labeling Standards. In that case, the ground displacement value was 1.5 times greater than that shown in Fig. 2 for both the original ground and the improved ground, while no modifications were made to the M–ϕ relationship for the pile bodies. In this case, based on the maximum ground surface response acceleration spectrum of 2.82 m/s² and the maximum displacement of 98 mm for the improved ground section obtained from the aforementioned seismic response analysis, another analysis using simulated seismic motion with a different phase yielded a maximum ground surface response acceleration spectrum of 2.03 m/s² and a maximum displacement of 75 mm. Therefore, the ratio between the maximum ground surface response acceleration spectrum and the maximum displacement was considered to be nearly identical.

3.3 Analysis Cases

To examine the relationship between the improvement area and the horizontal resistance of a static sand compaction pile, an analysis was conducted using the improvement area for the building described in Section 3.1 (improved ground section), as explained below. Cases A and B evaluate the impact of reducing the improvement area due to construction constraints, while Cases C and D evaluate the impact of reducing the improvement area to streamline the design. Figs. 7(a)–(d) illustrate the improvement areas and pile arrangements for each case.

・Case A: A situation where ground improvement cannot be implemented along two parallel boundaries to avoid impacts on adjacent land (Fig. 7(a)). In this case, the total number of piles installed in the improved ground section is 14, while 10 piles were installed in the unimproved ground section.

・Case B: A situation where ground improvement cannot be implemented along two perpendicular boundaries (Fig. 7(b)). In this case, the total number of piles installed in the improved ground section is 15, while 9 piles were installed in the unimproved ground section.

・Case C: A situation where ground improvement cannot be implemented at 4 corners (Fig. 7(c)). In this case, the total number of piles installed in the improved ground section is 20, while 4 piles were installed in the unimproved ground section.

・Case D: A situation where ground improvement cannot be implemented in the circumferential section (Fig. 7(d)). In this case, the total number of piles installed in the improved ground section is 8, while 16 piles were installed in the unimproved ground section.

・Case X: A situation where ground improvement is implemented for the entire area including directly beneath the building and in the circumferential section (original design). In this case, the total number of piles installed in the improved ground section is 24, while no piles were installed in the unimproved ground section.

In these cases, the unimproved ground section was assumed to have reduced improvement rates,

ensuring an F_L greater than 1.0 during Level 1 seismic motion, while allowing some layers in the section to undergo liquefaction with an F_L less than 1.0 during Level 2 seismic motion. Although a detailed examination, such as three-dimensional effective stress analysis, is required to accurately determine the layer susceptible to liquefaction, including the reduction in stiffness and the infiltration of excess pore water due to the liquefaction of the external ground and affected regions, this study simplifies these settings based on its purpose of assessing general tendencies and identifying future challenges.

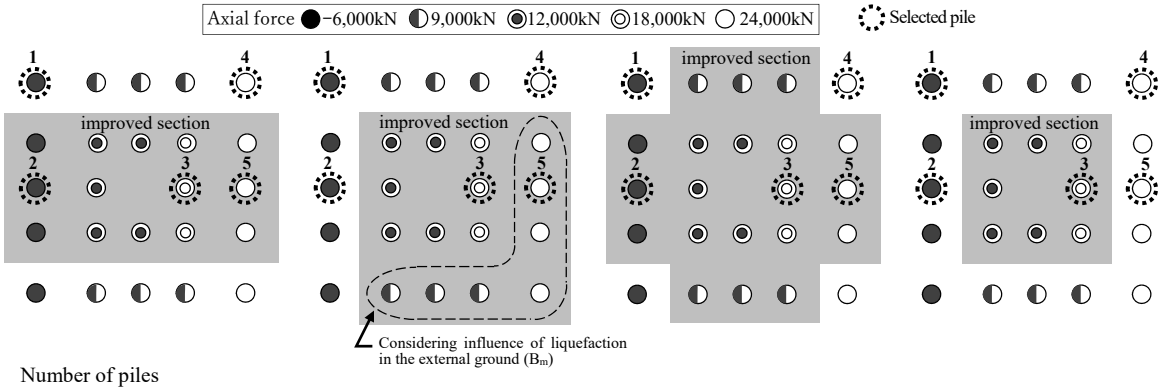

(a) Case A (b) Case B, Bc, Bm (c) Case C (d) Case D

Fig. 7 Analysis cases

4. ANALYSIS RESULTS

4.1 Comparison of Shear Force at Pile Head

With respect to shear force at the pile head Q_d of the selected piles analyzed in Cases A to D mentioned above, Figs. 8(a) and 8(b) present the results for Level 2 seismic motion and seismic motion 1.5 times greater than Level 2, respectively. The dashed lines in the figures represent the shear force distribution, assuming that the earthquake forces are equally borne by all piles.

The piles in the improved ground section (indicated in gray), which experienced a large ground reaction, exhibited concentrated shear forces at pile head (Q_d). In contrast, the piles in the unimproved ground section (indicated in white) were subjected to significant ground displacement, but each bore a shear force at pile head lower than the equalized shear force. In Case D, which featured a large unimproved ground section (with 16 piles in the unimproved ground section and 8 in the improved ground section), Pile No. 3, located in the improved ground section with a high axial force, bearing capacity, and significant ground reaction, experienced a shear force approximately twice the equalized shear force under Level 2 seismic motion. This highlights the fact that the load on the piles in the improved ground section increases as the size of the unimproved ground section grows. A similar situation was observed under seismic motion 1.5 times greater than Level 2, although the amplification relative to the equalized shear force was reduced due to the plasticization of the pile bodies.

Figure 8 shows the ratios (Q_d/Q_u) of shear force at the pile head (Q_d) for each pile to the safety limit shear force (Q_u) calculated using Eq. (3)[17]. In the equation, p_t is the tensile reinforcement ratio, F_c is the design standard strength of concrete, M/Qd is the shear span ratio, pw is the shear reinforcement ratio, σ_{wy} is a standard yield point of shear reinforcement, σ_0 is axial stress, b is the width of an equivalent rectangular cross–section, and j is the distance from the location of compressive stress resultant to the centroid of tension steel. However, the reduction constant[18], which accounts for the uncertainty of the capacity model, was not considered in the calculation.

$$Q_u = \left\{ \frac{0.053 p_t^{0.23} (18 + F_c)}{M/_{Qd} + 2} + 0.85\sqrt{p_w \sigma_{wy}} + 0.1\sigma_0 \right\} bj \tag{3}$$

Under Level 2 seismic motion, the piles in the improved ground section of Case D, which featured a larger unimproved ground section than the original design (indicated by □ in the figure), had Q_d/Q_u ratios greater than 1.0. Additionally, under seismic motion 1.5 times greater than Level 2, Piles No. 3 and No. 5, located in the improved ground section with high axial forces, had Q_d/Q_u ratios significantly exceeding 1.0, indicating that no safety margin was secured. Increasing the shear reinforcement from the original design of D13@150 (p_w = 0.9%) to D13@50 (p_w = 2.8%, as indicated by ● in the figure) allowed Q_u to almost exceed Q_d even under seismic motion 1.5 times greater than Level 2.

Accordingly, it was confirmed that the shear capacity of the piles in the improved ground section must be ensured when the improvement area is reduced, as these piles may experience large shear forces at the pile head due to the concentration of horizontal forces they are required to bear.

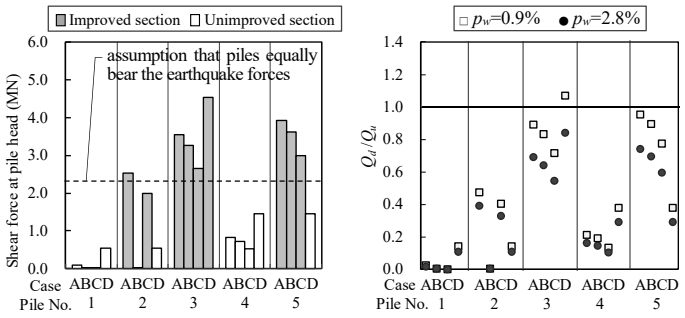

(a) Level 2 earthquake

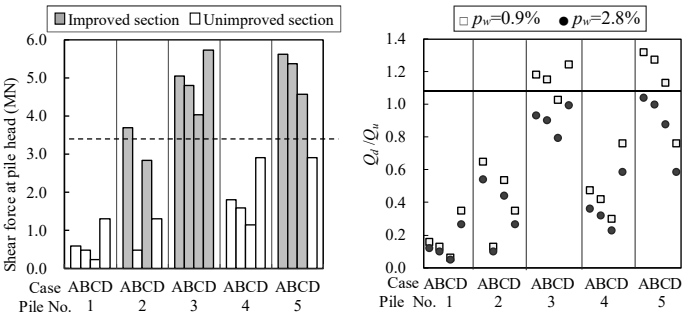

(b) Level 2 earthquake X 1.5

Fig. 8 Shear force at pile head Q_d and Q_d/Q_u

4.2 Comparison of Bending Moment between Cases Related to Construction Constraints (Cases A and B)

For Cases A and B, where the improvement area was reduced to account for adjacent land, Fig. 9 compares the bending moment distribution analyzed for Piles No. 1 to No. 5 with that of Case X, where the entire area underwent ground improvement. For Case B, since Piles No. 1 and No. 2 were located in the unimproved ground section and exhibited identical analysis conditions and results, only the bending moment distribution of Pile No. 1 is shown in the figure. Furthermore, Fig. 10 depicts the *M–N* interaction for each pile, illustrating the correlation between the pile head bending moment (*M*) and the axial force (*N*) borne by the pile, under seismic motion 1.5 times greater than Level 2.

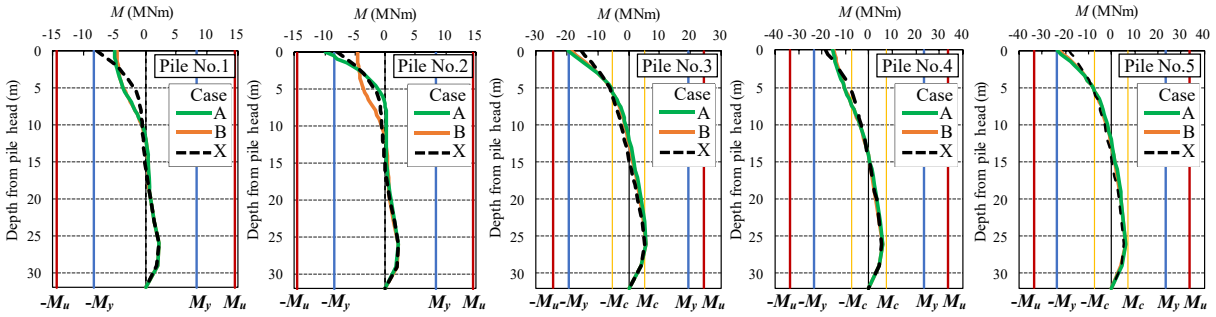

(a) Level 2 earthquake

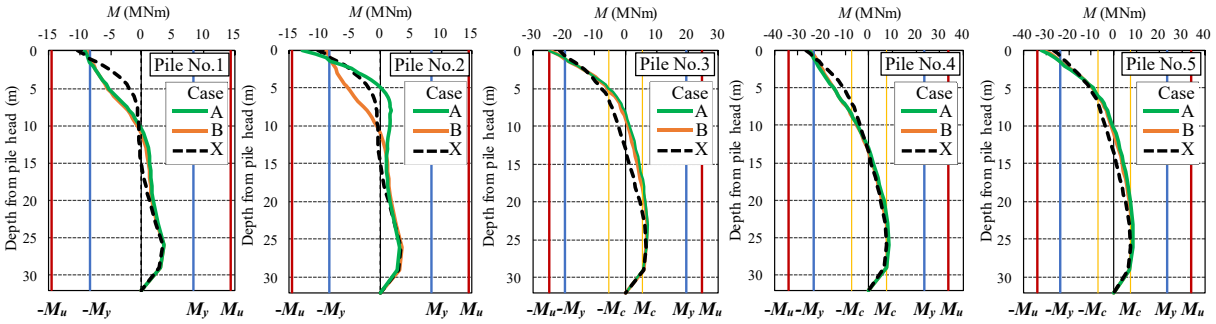

(b) Level 2 earthquake Χ 1.5

Fig. 9 Comparison of bending moment between cases related to construction constraints (Cases A and B)

In Cases A and B, the pile head bending moment of the piles in the improved ground section (Piles No. 3 and No. 5) exceeded that in Case X, while the pile head bending moment of the piles in the unimproved ground section (Piles No. 1 and No. 4) was lower than that in Case X. This trend corresponds to the distribution of shear forces at pile head described in Section 4.1. For Pile No.3 in the improved ground section, the pile head bending moment under Level 2 seismic motion was approximately equal to the yield bending moment (M_y), while under seismic motion 1.5 times greater than Level 2, it reached the ultimate bending moment (M_u). The bending moments of the other piles remained less than or equal to the ultimate bending moment (M_u).

In the original design, the centrally located Pile No. 1, which experienced small variations in axial force, had less main reinforcement compared to Pile No. 2, located along the perimeter, which was subject to significant pull–out forces during earthquakes. However, when the improvement area is reduced, Pile No. 1 is thought to require a reinforcement arrangement greater than or equal to that of Pile No. 2 to ensure safety under seismic motion 1.5 times greater than Level 2.

Additionally, except for Pile No. 2, which was subjected to different ground (improvement) conditions, the other piles showed small differences in bending moment indicating minimal influence of bearing capacity (axial force) on the horizontal force each pile needed to bear. The load distribution among the piles is primarily dependent on the number of piles in the improved and unimproved ground sections.

4.3 Comparison of Bending Moment between Cases Related to Design Streamlining (Cases C and D)

For Cases C and D, where the improvement area was reduced to streamline the design, Fig. 11 compares the bending moment distribution analyzed for Piles No. 1 to No. 5 with that of Case X, where the entire area underwent ground improvement. The trend in the distribution of bending moments as the external force increased was similar to that observed in Cases A and B. Therefore, the figure presents only the analysis results for the bending moments under seismic motion 1.5 times greater than Level 2. Additionally, Fig. 12 illustrates the *M–N* interaction for each pile, representing the correlation between the pile head bending moment (M) and the axial force (N) borne by the pile.

Compared to Cases A and B, Case C exhibited smaller differences in bending moments relative to Case X due to the higher proportion of piles in the improved ground section (20 out of 24). In contrast, in Case D, which had a smaller proportion of piles in the improved ground section (8 out of 24), the bending moments borne by the piles in the unimproved ground section were low. However, the overall trend was similar to that of Cases A and B, as evidenced by the fact that only Pile No. 3 in the improved ground section reached the ultimate bending moment (M_u).

Accordingly, it is considered that while the piles can maintain their bearing performance under Level 2 seismic motion even when the improvement area is reduced, the piles in the improved ground section near the central part of the building, where the burden of horizontal force is concentrated, may sustain damage as external forces increase. Therefore, when a structural element, such as a core wall designed to enhance seismic resistance, is centrally located, it is particularly important to determine the improvement area with careful consideration of the ratio of the number of piles in the improved ground section to those in the unimproved ground section.

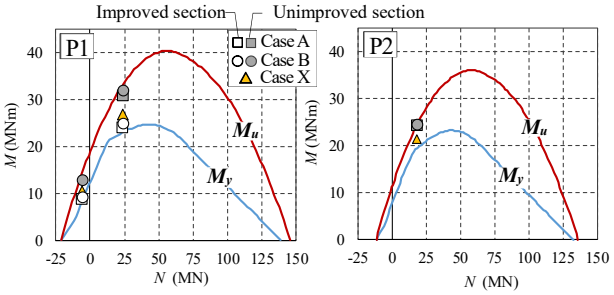

Fig. 10 *M–N* interaction at pile head(Case A, B, X)

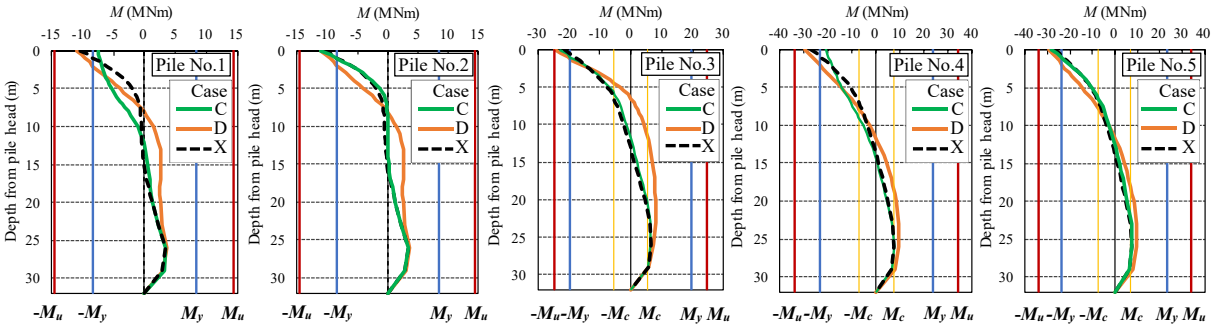

Fig. 11 Comparison of Bending Moment between Cases Related to Design Streamlining (Cases C and D) : seismic motion 1.5 times greater than Level 2

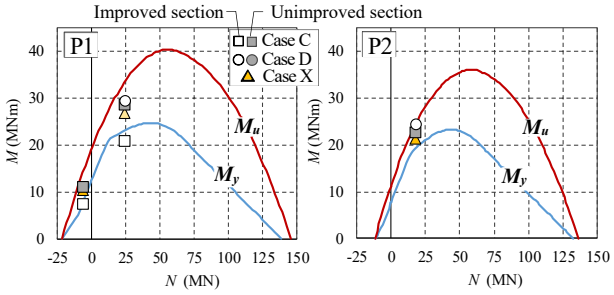

Fig. 12 *M–N* interaction at pile head (Case C, D, X)

4.4 Influences of Modeling the Improved Ground Section

The discussion in this paper is based on the fundamental assumption that the increase in subgrade reaction due to compaction is not considered for the improved ground section, and the effects of the unimproved ground section are also not considered. However, as discussed in Sections 4.1 to 4.3, in cases where improved and unimproved ground sections coexist, it was identified that the concentration of horizontal forces on the improved ground section requires particular attention when designing the improved ground section. Therefore, to examine the influence of differentiating the subgrade reaction setting in the improved ground section from the fundamental conditions on the horizontal resistance of the piles, additional analyses were conducted for cases in which increases in the subgrade reaction due to compaction were considered (subscript c). These cases included Cases B and D, which featured different sizes of improved ground sections, and Case X, where the improved ground section covered the entire area beneath the building. Additionally, Case B was re-analyzed (as Case Bm) by reducing the subgrade reaction to 0.5 or 0.6 to account for the influence of liquefaction in the external ground on the circumferential piles in the improved ground section, as illustrated in Fig. 7(b).

Figure 13 compares the bending moments on Pile No. 3 in the improved ground section and Pile No. 1 in the unimproved ground section under seismic motion 1.5 times greater than Level 2. In Case B, accounting for the effects of compaction caused the shear force at the pile head of Pile No. 1 in the unimproved ground section to decrease from 485 kN to 131 kN, leading to a corresponding reduction in the pile head bending moment. In contrast, Pile No. 3 in the improved ground section experienced an increase in shear force at the pile head from 4813 kN to 5052 kN, with almost no change in the bending moment. The same trend was observed in Case D, which had a smaller improved ground section. Additionally, Case X showed a slight decrease in the bending moment. This can be attributed to the fact that, in the improved ground section, the increase in shear force at the pile head was offset by the increase in the subgrade reaction, and the influence on the piles becomes greater with the increase in the subgrade reaction, given that the ground displacement remains constant.

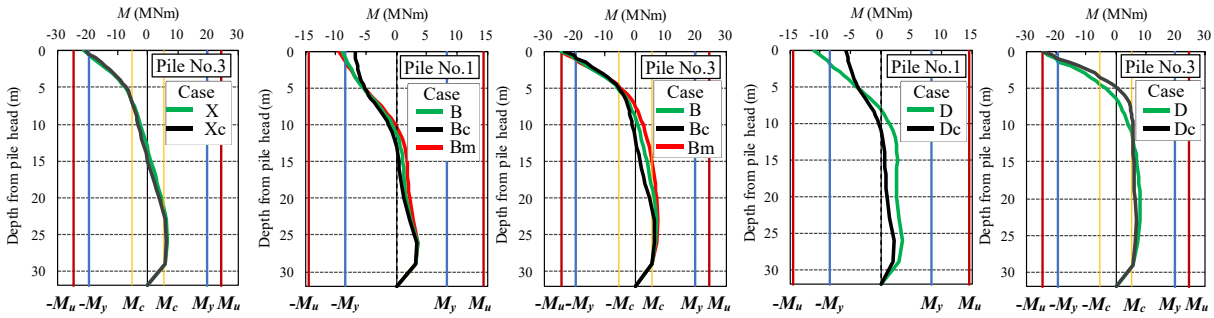

Fig. 13 Comparison of bending moment between cases related modeling of ground (Case X, B and D) : seismic motion 1.5 times greater than Level 2

Accordingly, if the increase in subgrade reaction due to compaction is not considered, a conservative evaluation can be made for the piles in the unimproved ground section, even in cases where the improved ground section covers the entire area beneath the building and both improved and unimproved ground sections coexist. However, it should be noted that the shear force on the piles in the improved ground section is underestimated. In contrast, an evaluation close to the safe side can be made for the bending moment. This can be attributed to the fact that the deformation modulus of the ground is increased in the improved ground section, which bears a larger pile head horizontal force due to the effect of compaction, resulting in a corresponding reduction in ground displacement. However, there may be cases where the rate of increase in the bending moment due to the concentration of the horizontal force exceeds the rate of reduction in the bending moment due to the effect of compaction. Therefore, if the safety margin for the bending moment is not sufficient, detailed analyses should be conducted, including comparative analyses of different possible combinations of the improved and unimproved ground sections.

Additionally, only one loading direction was considered in the discussion presented in this paper. While it is possible to estimate the behavior of piles under different loading directions based on the analysis results from this study, including the number of piles and the axial force (bending stiffness) experienced by each pile in both improved and unimproved ground sections. However, similar to what was described above, in order to ensure a sufficient safety margin for shear force or bending moment in the improved ground section, it is necessary to conduct analyses that explicitly account for multiple loading directions.

5. CONCLUSIONS

This study examined the influences of reducing the improvement area on the stresses generated on piles, focusing on the liquefaction countermeasure using the static sand compaction pile method. The analysis was conducted using a beam–spring model for cases where the improvement area cannot cover the entire area beneath a building due to construction or design constraints. As a result of the analyses, the key findings are summarized as follows:

・ This study examined the influences of reducing the improvement area in the liquefaction countermeasure using the static sand compaction pile method on seismic stresses affecting piles, evaluated the trends of these impacts, and identified relevant design considerations.

・Reducing the improvement area leads to a concentration of horizontal forces within the improved ground section, thereby increasing shear forces at the pile head and presenting a significant design challenge to ensure the shear strength of the piles in the improved ground section. Specifically, if the number of piles in the improved ground section is reduced to one-third of the total, the shear force at the pile head nearly doubles compared to a fully improved site (uniform bearing). Given the current lack of sufficient data on the deformation capacity of piles[18], careful design is essential to address the increased shear force at the pile head, including incorporating safety margins to prevent brittle fractures.

・The influences on bending moment remain relatively small, even when the horizontal force in the improved ground section increases due to a reduction in the improvement area. Meanwhile, the safety margin of the piles in the unimproved ground section is improved. However, the reinforcement arrangement for the piles in the improved ground section in the central part of a building must be carefully designed, as they experience increased pile head horizontal and shear forces during earthquakes, as well as a reduced safety margin for bending strength, despite experiencing minimal variation in axial force during earthquakes.

・Excluding the effects of compaction when modeling the horizontal subgrade reaction and calculating ground displacement does not always yield a conservative solution when improved and unimproved ground sections coexist. It is essential to note that shear force at the pile head tends to be underestimated in the improved ground section. In stress evaluations, the horizontal force, ground displacement, and subgrade reaction in the improved and unimproved ground sections can influence one another in different ways, depending on how they are combined. Therefore, when the safety margin is insufficient, it is crucial to analyze the stresses generated for each combination. Additionally, future challenges include developing a method for calculating ground displacement in infinitely continuous free ground that incorporates improved ground sections at dispersed locations.

This study focused on a single case of ground improvement under simplified examination conditions to evaluate the trends of its effects. It is necessary to further examine the trends by accumulating data in the future, setting precise examination conditions through effective stress analyses, and conducting analyses under various building and ground conditions to apply the findings to actual design.

REFERENCES

1) Architectural Institute of Japan: *Recommendations for Design of Ground Improvement for Building Foundations*, pp. 269–272, 2006.
2) Japanese Geotechnical Society: *Liquefaction Countermeasures*, pp. 221–297, 2004 (in Japanese,

title translated by the authors).
3) Architectural Institute of Japan: *Recommendations for Design of Building Foundations*, pp. 68–73, 2019.
4) Nozu, M. and Takeuchi, H.: Prediction of the Displacement of Surrounding Ground in the Implementation of the Static Sand Compaction Pile Method, *Proceedings of the 46th Geotechnical Symposium*, pp. 135–140, 2001 (in Japanese).
5) Architectural Institute of Japan: *Recommendations for Design of Ground Improvement for Building Foundations*, pp. 391–395, 2006.
6) Architectural Institute of Japan: *Recommendations for Design of Building Foundations*, pp. 13–22, 2019.
7) Architectural Institute of Japan: *Recommendations for Design of Ground Improvement for Building Foundations*, pp. 361–366, pp. 382–384, 2006.
8) Fire and Disaster Management Agency of the Ministry of Internal Affairs and Communications: Public Notice on the Details of Technical Standards Concerning the Regulations on Hazardous Materials, Ministry of Home Affair Notification No. 99, 1974 (in Japanese).
9) Tsuchida, H., Iai, S. and Kurata, E.: Area of Ground Compaction as a Measure against Liquefaction, *Presentation Summary of the 14th JSCE Earthquake Engineering Symposium*, pp. 9–12, 1976 (in Japanese, title translated by the authors).
10) Architectural Institute of Japan: *Recommendations for Design of Building Foundations*, pp. 50–58, 2019.
11) Kaneko, O., Kawamata, S., Nakai, S., Sekiguchi, T. and Mukai, T.: Analytical Study on Damage Factor of Pile Foundations During the 2011 off the Pacific Coast of Tohoku Earthquake, *Journal of Structural and Construction Engineering (Transaction of AIJ)*, Vol. 80, No. 717, pp. 1699–1706, 2015.
12) Mase, T. and Nakai, S.: Examination of Soil Spring Setting Method of Single Pile, *Journal of Structural and Construction Engineering (Transaction of AIJ)*, Vol. 77, No. 680, pp. 1527–1535, 2012 (in Japanese).
13) Architectural Institute of Japan: *Recommendations for Design of Building Foundations*, pp. 270–277, 2019.
14) Architectural Institute of Japan: *Recommendations for Design of Building Foundations*, pp. 27–34, 2019.
15) Japanese Geotechnical Society: *Geotechnical Investigation Method and Commentaries*, pp. 305–311, 2013 (in Japanese, title translated by the authors).
16) Yasuda, S. and Yamaguchi, I.: Dynamic Soil Properties of Undisturbed Samples, *Proceedings of the 20th Japan National Conference on Soil Mechanics and Foundation Engineering*, pp. 539–542, 1985 (in Japanese).
17) Architectural Institute of Japan: *Strength and Deformation Capacity of Foundation Structural Members*, pp. 75–77, 2022.
18) Architectural Institute of Japan: *Strength and Deformation Capacity of Foundation Structural Members*, pp. 38–39, 2022.

(Original Japanese Paper Published: November, 2024)
(English Version Submitted: March 12, 2025)
(English Version Accepted: April 26, 2025)